PAPER • OPEN ACCESS

Effect of pre-strain on microstructure and stamping ability of TA2 titanium alloy and H260 low-alloy steel

To cite this article: Po Liu *et al* 2023 *J. Phys.: Conf. Ser.* **2483** 012064

Effect of pre-strain on microstructure and stamping ability of TA2 titanium alloy and H260 low-alloy steel

Po Liu, Zhicheng Wen, Zhiguo Wang, and Zheng Liu*

School of Mechanical Engineering, Guilin University of Aerospace Technology, No.2 Jinji Road, Guilin, China

Corresponding author (Zheng Liu) Email: liuzheng@guat.edu.cn

Abstract. Applying pre-strain can not only change the microstructure and the mechanical property of metal material but also affect sheet metal stamping ability. In this paper, taking H260 low-alloy steel and TA2 titanium alloy as experimental materials, pre-strain ranging from 0 to 0.16 was applied using the one-step and the multi-step method respectively. Microstructure observation, tensile test, bending test, and cup bulging test were conducted on the pre-strained samples. Results show that in the pre-strain loading stage, the slipping and twinning deformation occurs in the TA2 alloy sample while dislocation sliding mainly happens in H260 low-alloy. With pre-strain increasing, the product of ultimate tensile strength and elongation rate gradually decreases, and the true ultimate tensile stress and accumulating elongation change rarely. The "product of yielding strength and elongation rate" can be enhanced by applying a pre-strain of 0.04 on the condition that plasticity is still at a high level. In the pre-strain range of 0 - 0.16, a bending test with a 30.8 °-opening angle can be completed on H260 steel. The springback angle changes from negative to positive with an increase in pre-strain. The bending ability of TA2 titanium alloy is very poor, for a crack can easily occur even in the original sample. The cupping value decreases gradually with an increase in pre-strain. The cupping value of TA2 titanium alloy is higher than that of H260 low alloy steel for the constant pre-strain. A quite large difference exists between the two experimental materials. Pre-strain loading pass has no significant effect on the microstructure evolution, mechanical properties, and stamping properties.

1. Introduction

Pre-strain is one of the important methods to change metal properties. For example, applying pre-strain can affect metal microstructure [1-2], strength [2-3], stiffness, creep property [4-5], fatigue property [6-7], forming performance [8], and so on. The reason for enhancing strength mainly lies that dislocation density increases and dislocation entanglement become worse after applying pre-strain. Twinning deformation happens more likely in the pre-strain loading stage for some hexagonal metals. After pre-straining, the yielding strength (σ_s) of a high-strength alloy is greatly enhanced while the ultimate tensile strength (σ_b) is less increased, and the elongation rate (*E*r) decreases rapidly due to the increase of yield ratio. Li et al. found out product of σ_b and *E*r changed rarely and is even slightly increased after pre-straining, which provides a new solution for adjusting the metal property. Pre-strain can bring in an effect on accumulating *E*r, namely the sum of pre-strain and *E*r of the pre-strained sample. However, the variation law of the accumulating *E*r with the constant pre-strain is not consistent due to different chemical components and preparation processes.

In sheet metal multi-step forming, work hardening caused by former pass deformation on the next pass can be regarded as an effect of pre-strain. The pre-strain can also influence springback behavior.

Therefore, strain hardening becomes a research hotspot in sheet multi-step forming, and it is listed as the key topic in the field of the effect of pre-strain on sheet forming performance in the 2011 NUMISHEET conference [10]. The forming limit of AAx610-T4PD aluminum alloy can be greatly improved by applying a pre-strain of 0.1 and the following intermediate annealing, according to the work by Zhang et al [11]. Pan et al. [12-13] studied the influence of pre-stretching and pre-compression on the cup bulging ability of the AZ31 magnesium alloy sheet. It was found that the base texture was gradually weakened and dispersed after pre-strain and heat treatment, which causes a high hardening index n value and increasing cupping value. Verma et al. [14] found that the bottom zone of the U-shaped part was permanently softened after pre-drawing and the elastic modulus was largely changed, which brings an effect on springback. Choi et al. [15] found that the springback amount of the U-shaped parts was greatly reduced after two-step bending, which was mainly attributed to the change of stress in the side wall. Chongthairungruang [16] and Yue et al. [17] found that the larger pre-strain led to a larger springback. Weiss et al. [18] found that bending yielding strength was reduced to a large extent based on the free bending experiment with pre-strained samples. At present, the effect of pre-strain on sheet stamping performance is still less systematically studied. Most pre-strain loadings were applied in a single-step way, and multi-step loading is required in certain deformation processes, such as drawing and multi-pass rolling. Since intermediate hardening or accumulating deformation will affect the final forming ability, enough attention should be put to the effect of pre-deformation in multi-step forming.

In this paper, H260 low-alloy steel and TA2 titanium alloy were used as the experiment material. A large range of pre-strain is loaded in single-step and multi-step methods to study loading pass and pre-strain value on microstructure. Besides, the effect of pre-strain on stamping performance is evaluated based on the v-shaped bending and bulging test, which provides a certain theoretical basis and research insight for property adjustment and sheet forming technique of high-strength alloy.

2. Experimental material and method

In this paper, the 1.2 mm thick annealed H260 low-alloy steel and the 1.2 mm thick annealed TA2 titanium alloy sheet were used. Microstructures of the original material were shown in Figure 1. The original microstructure of H260 is composed of the mainly equiaxed ferrite grain and a small amount of pearlite. The TA2 titanium alloy is composed of an equiaxed α phase.

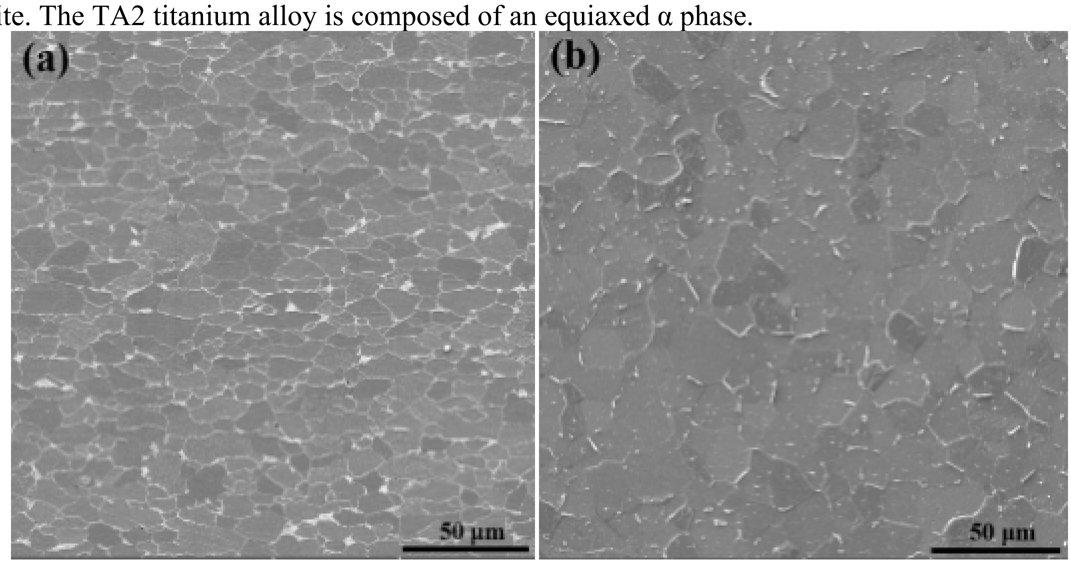

Figure 1. Microstructure of original material of (a) H260 low alloy steel and (b) TA2 titanium alloy

Two kinds of tensile specimens were cut along the rolling direction, namely one with standard gauge width of 12.5 mm (standard gauge SG) and the other with wide gauge width of 60 mm. The parallel section length is 62.5 mm, as shown in Figure 2. By using the electronic universal testing machine, the two specimens were previously loaded to strains of 0.04, 0.08, 0.12, and 0.16, respectively. The velocity was 3 mm/min and the extension gauge length was 50 mm. Then, tensile tests were carried out on the pre-strained SG samples. The test ended when the load decreased by 10% in the necking stage. The elongation in this situation was calculated as elongation rate (*E*r). To study the influence of multi-step pre-deformation on deformation ability, two-step pre-loading with 0.04 + 0.04 and 0.04 + 0.08 were used, corresponding to the accumulated strain of 0.08 and 0.12 respectively. Three-step loading with 0.04 + 0.04 + 0.04 was applied, corresponding to the accumulated strain of 0.12. Each kind of tensile test was repeated three times to avoid statistical error.

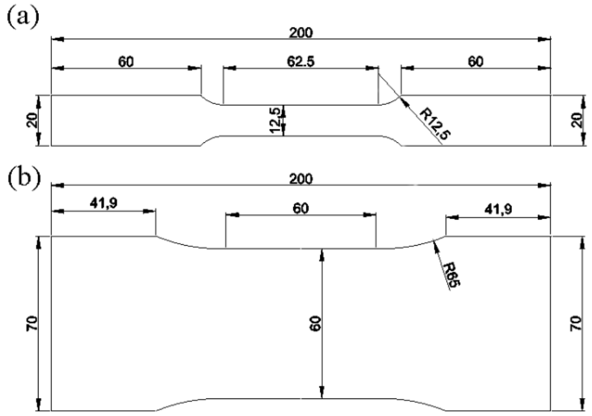

Figure 2. Geometric illustration (in mm) of specimens used in tensile tests (a) with standard gauge and (b) wide gauge

The samples were cut along a tensile direction for microstructure observation. They were ground and polished consecutively. After that, H260 samples were etched with 4% nitrate alcohol and TA2 samples with HF: HNO3: H2O = 1: 3: 100 (volume ratio) solution. The longitudinal section was observed by optical microscope and scanning electron microscope (SEM). The samples were mechanically thinned and ionic thinned to obtain a Φ3 mm wafer used for microstructure analysis by using transmission electron microscopy (TEM).

The v-shaped bending test was carried out on the pre-strain SG sample. The die opening angle was 30.8 ° and the punch fillet radius was 0.5 mm. A cupping test was performed on the pre-strained WG sample with a punch speed of 6 mm/s. The punch radius was 20 mm and the blank holder force was 98 KN.

3. Results and Discussion

3.1 Effect of pre-strain on microstructure

The TEM microstructure of the original H260 sample is shown in Figure 3. It can be seen there are a few dislocations in α ferrite grains and annealing twins exist in several α-Fe grains, which shows that relatively full recrystallization is completed after annealing. In the pre-strain loading stage, dislocation sliding is initiated, and dislocation density increases with pre-strain increasing. Meanwhile, more sub-grains are generated, of which the boundary is composed of a dislocation wall. Although annealing twins exist in the original microstructure, they rarely take part in plastic deformation. Dislocation slipping is the main deformation mechanism for α ferrite, as shown in Figure 4.

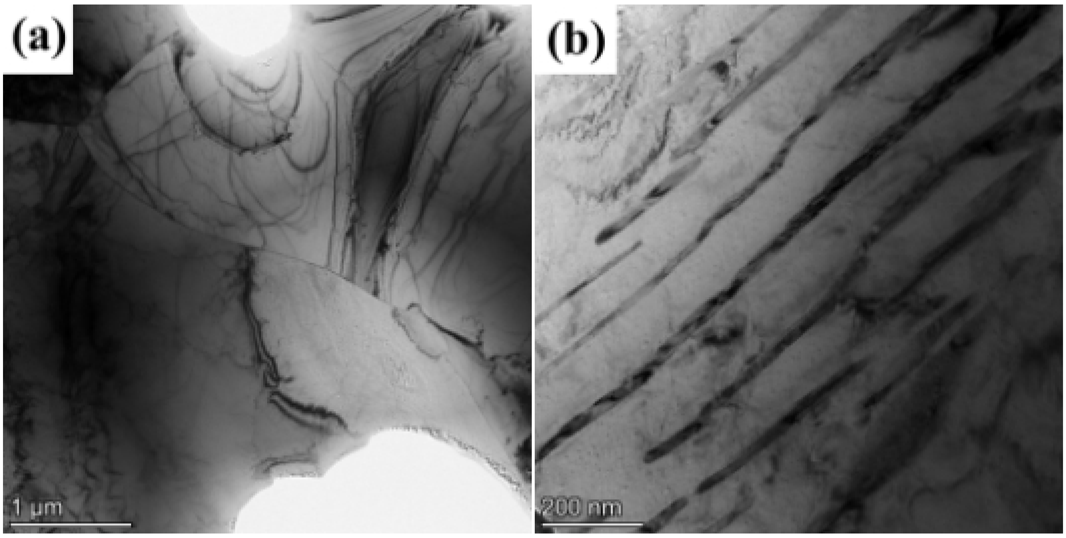

(a) NO 1 region, (b) NO 2 region
Figure 3. Microstructure of the H260 original specimen

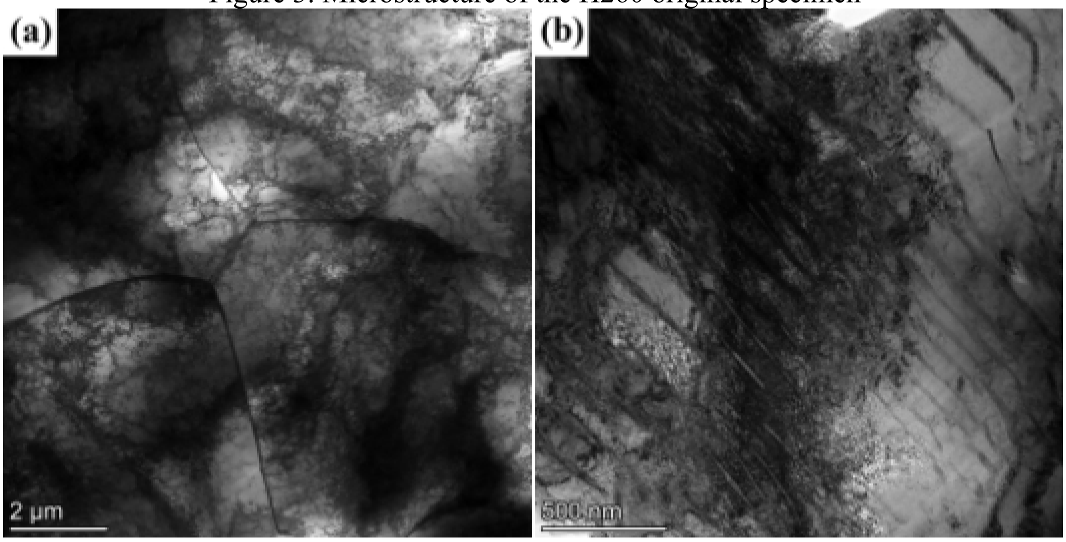

(a) NO 1 region, (b) NO 2 region
Figure 4. Microstructure of the 0.08 pre-strained H260 specimen

Figure 5 shows the TEM microstructure of the original TA2 sample. Based on the SEM (seen in Figure 1(b)) and TEM microstructure, a certain number of annealing twins exist in the original TA2 sample, and a few dislocations appear in the α phase. The microstructure of the 0.08 pre-strained sample is shown in Figure 6. The amount of the deforming twin increases in the α phase, and large dislocation walls appear. When the larger pre-strain is applied, these dislocation walls will transform into the sub-grain boundary.

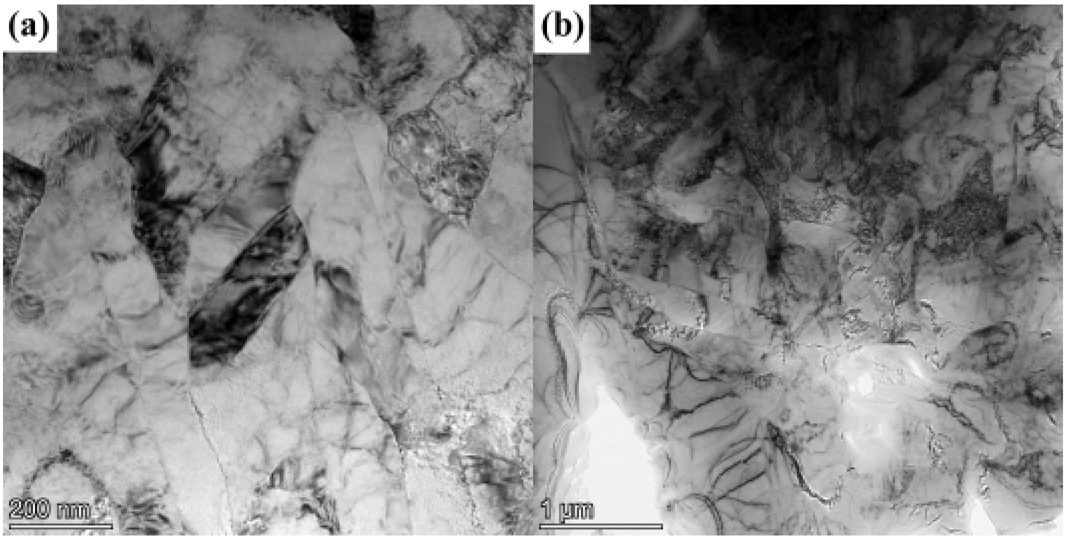

(a) NO 1 region, (b) NO 2 region

Figure 5. Microstructure of original TA2 specimen

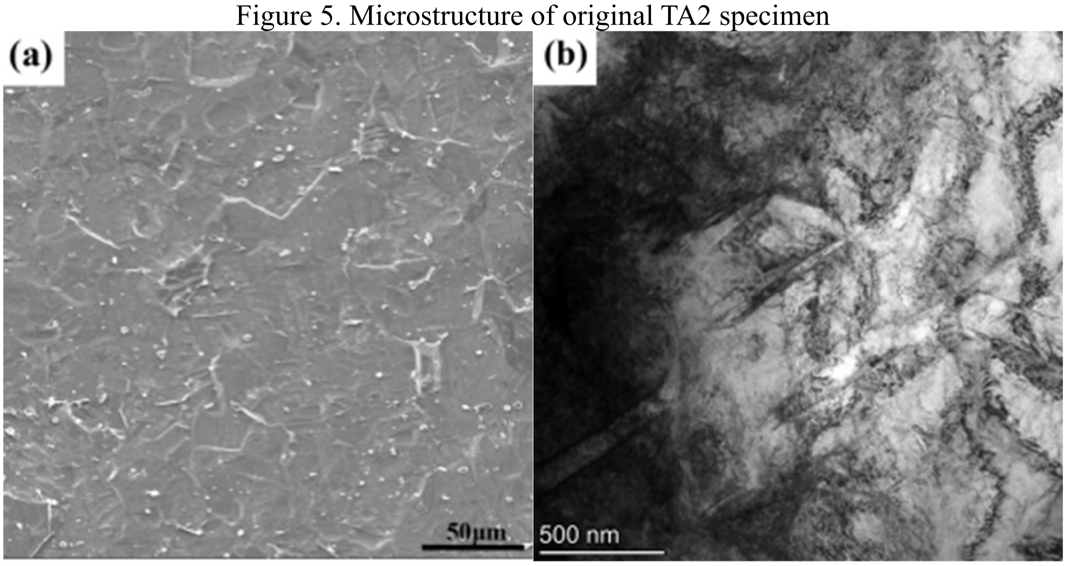

Figure 6. The (a) SEM microstructure and (b) TEM microstructure of the 0.08 pre-strained TA2 titanium alloy specimen

3.2. Influence of pre-strain on mechanical property

Figure 7 describes the variation law of the mechanical property of H260 and TA2 samples with single-step pre-strain. With pre-strain increasing, both σ_s and σ_b of each material increase, and Er decreases gradually, which is consistent with the result of many research works [3,9,19]. Nominal stress and strain cannot reflect the real condition at the large deformation stage, so mechanical property indexes such as true yielding strength $\sigma_{s\text{-true}}$, ultimate tensile strength $\sigma_{b\text{-true}}$, and true yield ratio are calculated based on true stress and strain data. The variation curves of $\sigma_{s\text{-true}}$ and $\sigma_{b\text{-true}}$ with pre-strain are shown in Figure 7(b). $\sigma_{b\text{-true}}$ of H260 specimens changes rarely and $\sigma_{s\text{-true}}$ gradually increases with pre-strain. A similar phenomenon is also observed in TA2 titanium alloy. However, when the pre-strain is larger than 0.12, $\sigma_{s\text{-true}}$ and $\sigma_{b\text{-true}}$ of TA2 titanium alloy are quite close. From the perspective of real stress and strain, the true yield ratio of the H260 sample is significantly lower than its nominal yield ratio, and so it is the TA2 titanium alloy. As for the same pre-strain, the yield ratio of H260 low alloy steel is smaller than that of TA2 titanium alloy, which means that H260 low alloy steel can endure larger plastic deformation. When the pre-strain value is larger than 0.08, the yield ratio of TA2 titanium alloy reaches 1. Therefore, such alloy faces a high risk of failure when it is previously loaded with a strain larger than 0.08. The *E*r decreases rapidly with an increase in pre-strain for each material, as shown in Figure 7(d).

Stretching deformation on the pre-strain sample can be considered as two-step loading on the original sample. Therefore, the total elongation rate can be expressed as a sum of the pre-strain and *E*r of the pre-strained sample [9]. It can be seen from Figure 7(d) that the total elongation rate is quite close at each pre-strain The reason is that the tensile plasticity of pre-strained specimens is reduced by the higher dislocation density, which is consistent with many research works [3,9]. It is reported in reference [20-21] that the total elongation rate of St15 cold-rolled automotive steel and the 5754 aluminum alloy plate increased after they are previously pre-loaded to the strain of 0.17. The reason lies that the hardening index *n* of the two pre-strained samples is higher, and the large elongation rate can be maintained before reaching the ultimate tensile stress. Generally, the influence of pre-strain on the total nominal strain is tiny. The total elongation rate of the sample is still consistent with that of the original material, even at high pre-strain (such as 0.12 and 0.16). This is different from multi-step deep drawing used to obtain a smaller drawing ratio and multi-pass rolling used to obtain a larger reduction. The purpose of multi-step deep drawing is to avoid excessive stretching force in the cup wall, so the total drawing ratio is less than that of single-step deep drawing. Multi-pass rolling can yield a large total deformation with a small rolling force and a small dislocation density [22], so a larger amount of rolling reduction can be achieved.

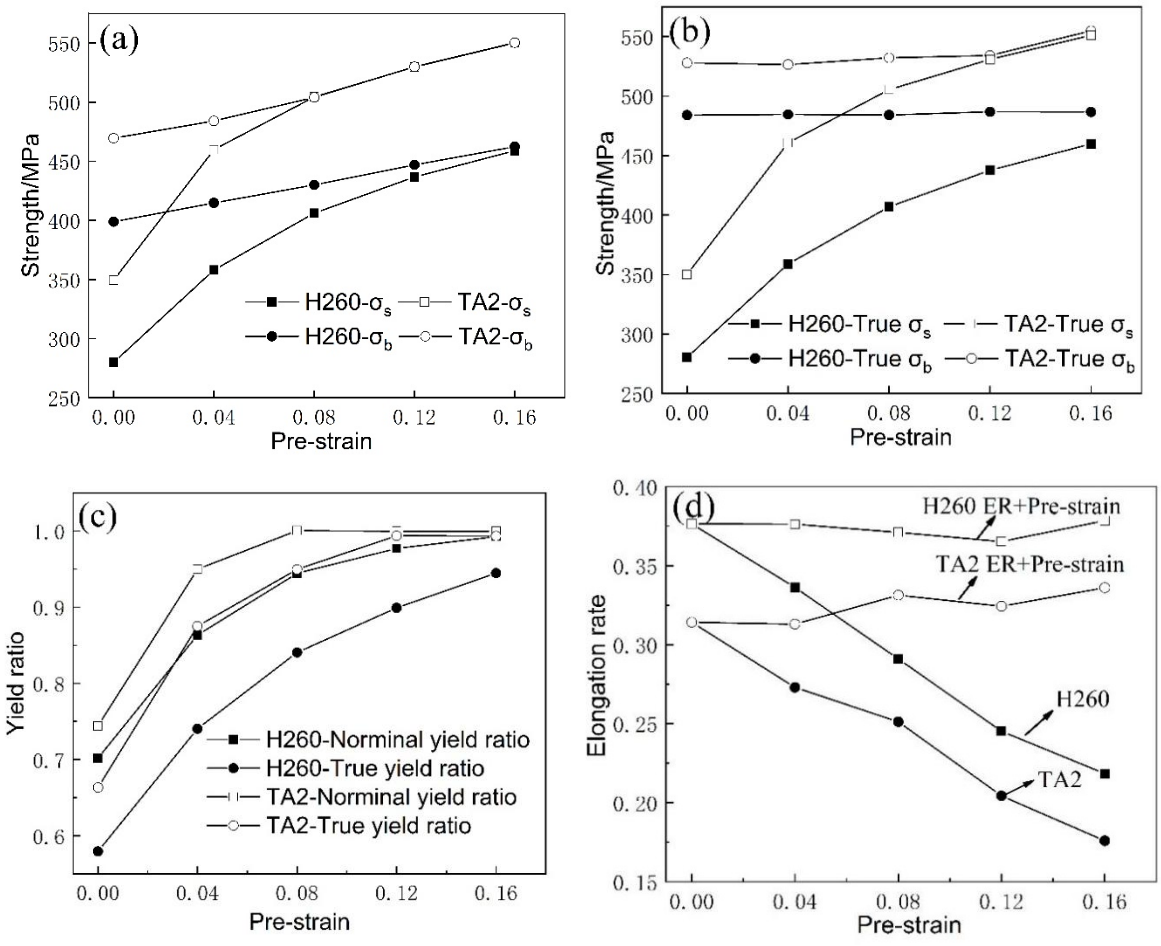

(a) nominal YS and UTS, (b) true YS and UTS, (c) nominal and true yield ratio, (d) elongation rate
Figure 7. Variation curve of several properties with pre-strain of H260 steel and TA2 titanium alloy

The product of σ_b and *E*r reflects work to pulling out the specimen, and it is also the comprehensive evaluating index for the metal strength and toughness. The variation of the product of σ_b and *E*r with pre-strain is shown in Figure 8. $\sigma_b \times E$r product decreases gradually with pre-strain. It is mainly due to the increase in tensile strength caused by pre-strain being less than the decrease in elongation, as shown in Figures 7(a) and (b). The product of σ_s and Er can be used to express the ultimate redundancy degree of metal deformation failure. Thus, it can be defined as a product of yield strength and elongation rate. As can be seen from Figure 8, the $\sigma_s \times E$r of TA2 titanium alloy at a pre-strain of 0.08 and H260 high-strength steel at a pre-strain of 0.04 reached the peak respectively, and then they gradually decreased. When pre-strain is 0.12, the $\sigma_s \times E$r product is reduced to that of the original specimen. Besides, the yield ratio of the TA2 specimen reaches 1 when the pre-strain is 0.08 leaving a very limited deformation room. From above, the higher proper $\sigma_s \times E$r can be achieved by applying a pre-strain of 0.04 for the two materials, in which situation the yield strength is increased by 30% and plasticity is only reduced by 10.6%.

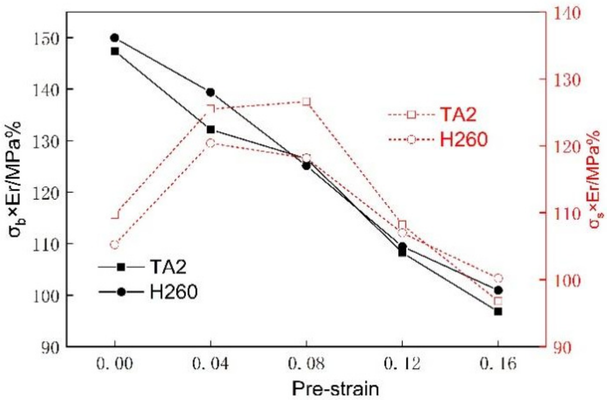

Figure 8. Variation curves of production of yielding strength/ ultimate tensile strength and elongation with pre-strain for TA2 titanium alloy and H260 steel

The mechanical property of specimens with two-step (0.04 + 0.04) and (0.04 + 0.08) loading and with three-step (0.04 + 0.04 + 0.04) loading was statistically summarized in Table 1 and Table 2. When the total pre-strain is equal, there is a very tiny change in yield strength, ultimate tensile strength, hardening index, elongation rate, and total Er of the multi-step pre-strained specimens. Such property parameter is nearly equal to that of the single-step loading with the same pre-strain.

Table 1. Property parameter of TA2 specimens with multi-step pre-strain

Pre-strain	σ_s/MPa	σ_b/MPa	n	Er	Total Er	$\sigma_s \times E$r /MPa%
0	349.4	469.4	0.137	31.4%	31.4%	147.4
0.08	504.3	504	0.046	25.1%	33.1%	126.5
0.04+0.04	503.66	504.6	0.049	23.6%	31.6%	119.1
0.12	529.7	529.88	0.035	20.43%	32.43%	108.25
0.04+0.04+0.04	529.1	529.22	0.038	22.89%	30.9%	121.1

Table 2. Property parameter of H260 specimens with multi-step pre-strain

Pre-strain	σ_s/MPa	σ_b/MPa	n	Er	Total Er	$\sigma_s \times E$r /MPa%
0	279.92	398.8	0.195	37.6%	37.6%	149.95
0.08	406.08	429.99	0.073	29.1%	37.1%	125.13
0.04+0.04	404.13	429.46	0.075	28.1%	36.1%	120.68
0.12	436.7	446.9	0.058	24.5%	36.5%	109.45
0.04+0.08	435.87	445.77	0.057	24.9%	36.9%	111.00
0.04+0.04+0.04	434.82	445.55	0.058	25.2%	37.2%	112.28

3.3. Influence of pre-strain on stamping performance

The H260 and TA2 bent samples with different pre-strain are shown in Figure 9. As can be seen from Figure 9(a), All bending trials of the H260 sample can be successfully completed and no cracks are observed in the outer surface, regardless of pre-strain value and loading pass. For TA2 titanium alloy, the crack easily occurs even using original specimens. Moreover, crack still happens when using the die with an opening angle of 88 ° instead, as shown in Figure 9(b). The difference in bending ability of such two materials is very large, which is due to TA2 pure titanium possessing lower plasticity and higher yield ratio. The outer surface of this sample quickly reaches ultimate stress at small bending deformation. Thus, TA2 titanium alloy has poorer bending ability than H260 low alloy steel.

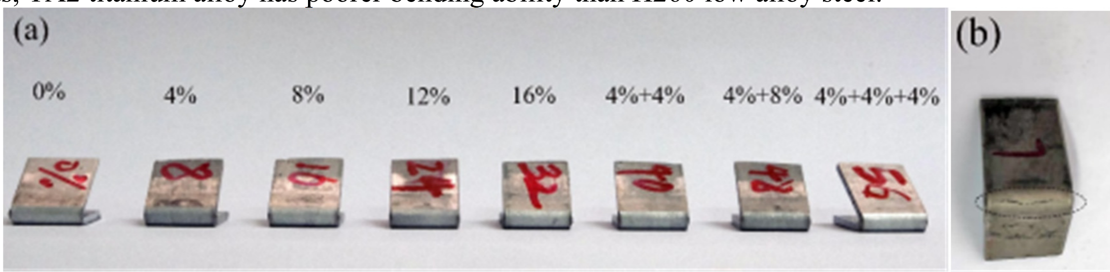

(a) H260 steel specimens with different pre-strain, (b) TA2 titanium alloy specimen with 88°-opening angle punch

Figure 9. The bent specimens of H260 and TA2 titanium alloy

The springback angles of H260 samples with different pre-strain are listed in Table 3. The springback angle gradually turns from a negative to a positive value with pre-strain. Moreover, the positive springback angle keeps continuously increasing. The negative springback angle is obtained when applying a pre-strain of 0 - 0.04. It is attributed to the small punch radius. An arc of small curvature is formed in the transition zone near the end of the bending stage, and this arc is straightened at the final stage [23-24]. Upon unloading, the internal bending moment in this region forces the specimen to turn inward. Moreover, the inner bending moment is larger than the moment in the bending area. Consequently, the specimen turns inwardly under the complicated action of the bending moment in a different area, and the negative springback angle is finally achieved [25]. It is known that the bending moment is linearly related to the yield strength, the bending moment in the deformation zone increases correspondingly. Therefore, a positive sprinback angle is obtained when the pre-strain is greater than 0.08 and it gradually increases with pre-strain.

The springback angle of the pre-strained samples with two-step (0.04 + 0.04) loading is close to that with single-step pre-strain 0.08 loading. Similarly, the springback angle of the pre-strained sample with two-step (0.04 + 0.08) and three-step (0.04 + 0.04 + 0.04) loading is close to that with single-step pre-strain 0.12 loading. It implies that the loading step causes a very limited effect on the springback of H260 as long as the total strain in multi-step loading is equal to that in single loading.

Table 3. Springback angle of H260 specimens with different pre-strain

Pre-strain	0	0.04	0.08	0.12	0.16	0.04+0.04	0.04+0.08	0.04+0.04+0.04
springback/°	-3.50	-1.71	1.48	3.07	4.20	1.29	3.3	3.71

Figure 10 shows the variation curve of cupping value and comprehensive deformation of H260 steel and TA2 titanium alloys with pre-strain in a single-step loading method. It can be seen that the cupping value decreases continuously with pre-strain. As for the original and slightly pre-strained specimens, the cupping value of TA2 titanium alloy is higher than H260 steel, showing that TA2 alloy yields a better thinning resistance ability. With an increase in pre-strain, the cupping value of TA2 alloy decreases rapidly and it then reduces to equal to that of H260 steel at a pre-strain of 0.16. The better bulging ability of TA2 is due to that equiaxed grains can tolerate large thinning. With pre-strain increasing, the TA2 grains maintain their primary shape and they are rarely elongated, as shown in Figure 6. However, dislocation density increases in the TA2 pre-strained specimens, and the {111} texture beneficial in stamping decreases, and other textures harmful to stamping ability increase [26], resulting in a rapid decline in *I*e value.

In fact, the WG sample has undergone uniaxial tensile elongation and cup bulging deformation, it is proper to use comprehensive deformation amount to evaluate accumulating deformation degree. The comprehensive deformation is represented by the sum of the ratio of the pre-strain to the original specimen *E*r and the ratio of the cupping value of the pre-strained sample to that of the original one. It can be seen from Figure 10(b) that the comprehensive deformation gradually increases with pre-strain. It is ascribed to the increase in the proportion of the pre-stretch deformation is much higher than the decrease in the relative cupping value of the pre-deformed specimens. In contrast between a decrease in *E*r and in the cupping value of the two materials, as shown in Figure 7(d) and Figure 10(a), pre-strain can cause a much larger influence on *E*r than the cupping value. It is mainly due to the higher dislocation density caused by pre-strain loading weakens the unidirectional elongation ability and has a limited effect on bulge thinning ability. It is shown in reference [27] that the plastic strain ratio r value of H300 low-alloy high-strength steel gradually increases to peak with pre-strain at 0.09 and then slowly decreases. It implies that the increasing r value can inhibit the rapid decline of the cupping value. The high r value is one of the reasons for a slow decline in the cupping value of H260 steel pre-strained specimens.

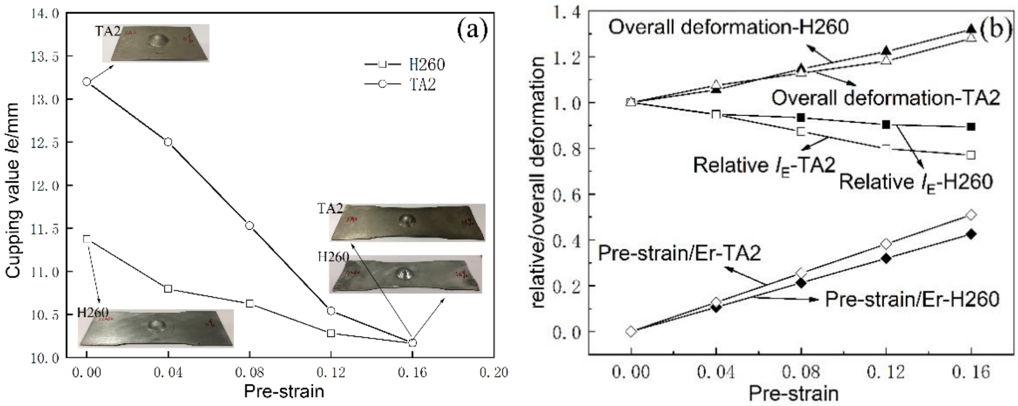

Figure 10. Variation curve of (a) cupping value and (b) overall deformation of H260 steel and TA2 titanium alloy specimens with pre-strain

3.4. Analysis and Discussion

TA2 titanium alloy has less slip system than H260 low-alloy steel, thus slip and twinning is the main deformation mechanism in the pre-strain loading stage as for the former material, in which twinning is triggered by stress concentration due to dislocation pile-up, as shown in Figure 6. Twinning deformation accounts for a proportion of contribution less than 10% in total deformation. However, the orientation of the twinning grain changes, and it in turn promotes slip deformation. Since the tensile samples were cut along the sheet rolling direction, slipping is difficult in the base plane of HCP-structured TA2 titanium alloy, while it is feasible for the cylinder plane. Consequently, the deformation twinning textures are mainly {1012} and {1121}[28]. Except for twin sliding deformation, α grain rotation also takes part in plastic deformation, namely dislocation walls caused by early slip deformation and another low-energy dislocation form into sub-grain. Under the action of activation and axial stress, these sub-grains merge into a large sub-grain with a high-angle grain boundary (HAGB), and the sub-grain with a low-angle grain boundary merged into large grain through grain boundary rotation. Such formed grains can play a role in coordinating deformation, thus reducing stress concentration in the grain boundary and improving plastic deformation ability [26]. The SEM microstructure of the 0.08 pre-strained TA2 sample is consistent with the original microstructure, as shown in Figure 6 (a)), which indirectly proves the analysis of the conclusion above. Because the threshold shear stress for dislocation slipping of H260 low-alloy steel is small, dislocation slip mainly occurs in the pre-strain loading stage, and the twinning hardly occurs. More and more sub-grains are generated with pre-strain increasing. In addition, the necking area and its adjacent region endure large plastic deformation when it reaches the ultimate tensile stress. Grains in such areas are thus elongated to a certain extent.

As discussed above, TA2 titanium alloy has a higher r-value. Since the feasible sliding system distributes in crystal face and orientation angle between c axis and sheet normal direction, the rapid thinning of the plate is inhibited, and the highest r value is obtained for the TA2 original samples. In the pre-strain loading stage, slipping proceeds mainly along the <1120> direction parallel to the base plane. In addition, the orientation angle between the c-axis and the sheet's normal direction is changed due to grain rotation. It is generally believed that the r value decreases gradually with the increase of deformation amount, and high dislocation density leads to an increase in yield ratio and a decrease in n value. In general, the r value is an important factor affecting plane-forming ability. Therefore, the higher *r* value and the intact even grain are the reason why the cupping value of the pre-strained TA2 sample is higher than H260 steel.

Bending ability is related to fillet radius, thickness and die opening angle. It was reported in reference [29] that a bending test using a fillet radius of 0.5 mm and an opening angle of 90 ° were successfully conducted on a 0.5 mm thick commercial pure titanium plate at room and medium temperature. However, a crack occurred on the 4 mm thick pure titanium plates when subjected to a three-point bending test at a high temperature [30]. It indicates that the relative bending radius has a great influence on bending performance. The thinning degree of the bending zone increases with a decrease in the relative bending radius. The bending layer thinning of the TA2 titanium alloy sheet is greatly inhibited due to the high r-value. Combined with a high yield ratio and low hardening index, a crack happens early on the outer layer of TA2 titanium alloy when it experiences small plastic deformation. The H260 pre-strained specimen still has a relatively high elongation rate and low yield ratio, which ensures that the outer surface can withstand a certain amount of tensile elongation. In addition, the transition zone participates in bending deformation due to good plasticity at room temperature, which reduces deformation in the bending zone to a certain extent. Therefore, the bending ability of H260 low alloy steel is much better than TA2 titanium.

As for each test like pre-strain loading, tensile deformation, bending, bulging, and so on, intermediate annealing was not applied to the samples. Thus, the influence of work hardening in multi-pass loading cannot be eliminated. Besides, the subsequent yield effect is tiny in multi-step loading, and the hardening effect is basically the same as that in single-step loading. Therefore, the influence of loading pass on microstructure and property is slight. The microstructure evolution and property change are mainly dependent on the accumulating deformation amount [31].

4. Conclusion

The pre-strain deformation of TA2 alloy is mainly dominated by slip and twinning. However, the TA2 alloy grain shape hardly changes with pre-strain increasing. The degree of ferrite grain elongation of the H260 steel sample increases with pre-strain. Dislocation slip and sub-grains generation mainly occur in the pre-tensile deformation of H260 steel.

With the increase of pre-strain, the yield strength of H260 low-alloy steel and TA2 titanium alloy increases rapidly. Nevertheless, the increasing tendency of tensile strength is not obvious. *E*r and *n* gradually decrease, and the yield ratio gradually increases to 1. Under the constant pre-strain, the strength and yield ratio of TA2 titanium alloy is higher than H260 steel, while the elongation rate and hardening index are lower than H260 steel. The accumulating elongation rate of each material changed little with pre-strain and tended to be equal. The product of $\sigma_b \times E$r decreases with pre-strain. When the pre-strain is 0.04, the higher proper product of $\sigma_s \times E$r can be obtained for each metal, compared to the original one, on the condition that yield strength can be promoted by 30% while plasticity is only reduced by 10.6%.

The poor bending performance of TA2 titanium alloy is related to the high r-value and yield ratio. H260 low alloy steel has excellent bending performance, and the bending experiment can be successfully completed on the highly pre-strained specimens. The springback angle changes from negative to positive with pre-strain. The cupping value decreases with pre-strain for each material. At the constant pre-strain, the cupping performance of TA2 titanium alloy is better than H260 steel. After pre-strain loading and cup bulging, the comprehensive deformation increases gradually with pre-strain. The effect of pre-strain on the reduction of elongation rate is much greater than that of cupping value.

The mechanical and stamping performance of the specimen with multi-step pre-strain is basically equal to those of the single-step pre-strained specimen. The influence of loading pass on microstructure and property is not obvious.

Acknowledgments
This work is supported by the Natural Science Foundation of Guangxi Zhuang Autonomous Region (NO:2020JJA160034) and the Basic ability improvement of Middle and Young teachers in Guangxi Universities Foundation (NO:2020KY21018)

References
[1] Ren P, Chen XP, Wang CY, et al. 2022 Effects of pre-strain and two-step aging on microstructure and mechanical properties of Fe-30Mn-11Al-1.2C austenitic low-density steel. *Acta Metall. Sin*. **58**(6) 771
[2] Quan L W, Zhao G, Sam G, et al. 2011 Effect of pre-stretching on the microstructure of aged 2524 aluminium alloy. *Trans. Nonferrous Metal. Society of China* **21**(09) 1957
[3] Li KS, Peng J, Peng J, et al. 2018 Influence of pre-strain on the mechanical behavior of Austenitic stainless steel and construction of constitutive models. *Mater. Eng*. **46**(11) 148
[4] Jang MH, Kang JY, Jang JH, et al. 2018 Microstructure control to improve creep strength of alumina-forming austenitic heat-resistant steel by pre-strain. *Mater. Charact*. **137** 1
[5] Xiao ZY, Huo QH, Zhang ZR, et al. 2019 Influence of pre-straining on creep behaviors of Mg-2Y alloy sheets. *J. Alloy. Compd.* **806** 19
[6] White BC, White RE, Jordon JB, et al. 2018 The effect of tensile pre-straining on fatigue crack initiation mechanisms and mechanical behavior of AA7050 friction stir welds. *Mater. Sci. Eng. A* **736** 228
[7] Dai Q, Wang F, Zang J, et al. 2020 Effect of pre-strain on failure assessment of titanium pressure vessel with crack. *Rare Metal Mater. Eng.* **49**(10) 3301
[8] Han L, Young KW, Chrysanthou A, et al. 2006 The effect of pre-straining on the mechanical behavior of self-piercing riveted aluminium alloy sheets. *Mater. Des.* **27**: 1108
[9] Li ZC, Misra RDK, Ding H, et al. 2018 The significant impact of pre-strain on the structure-mechanical properties relationship in cold-rolled medium manganese TRIP steel. *Mater. Sci. Eng. A* **712** 206
[10] Li XQ, Dong HR, Yu CW, et al. 2020 Influence of yield criteria and hardening model on draw-bending springback prediction of DP780. *J. Mech. Eng.* **56**(12) 42
[11] Wang KF, Carsley JE, Zhang LH, et al. 2014 Forming limits of an age hardenable aluminum sheet after pre-straining and annealing. *Int. J. Mech. Sci.* **82** 13
[12] Yang QS, Jiang B, Song B, et al. 2022 The effects of orientation control via tension-compression on microstructural evolution and mechanical behavior of AZ31 Mg alloy sheet. *J. Magnesium Alloy.* **10**(2) 411
[13] Dong JR, Zhang DF, Dong YF, et al. 2014 Microstructure evolution and mechanical response of extruded AZ31B magnesium alloy sheet at large strains followed by annealing treatment. *Mater. Sci. Eng. A* **618** 262
[14] Verma RK, Chung K, Kuwabara T. 2011 Effect of pre-strain on anisotropic hardening and springback behavior of an ultra-low carbon automotive steel. *ISIJ Int.* **51**:482
[15] Choi J, Lee J, Bong HJ, et al. 2017 Advanced constitutive modeling of advanced high strength steel sheets for springback prediction after double stage U draw bending. *Int. J. Solids Struct*. **151**: 152
[16] Chongthairungruang B, Uthaisangsuk V, Suranuntchai S, et al. 2012 Experimental and numerical investigation of springback effect for advanced high strength dual phase steel. *Mater. Des*. **39** 318

[17] Yue ZM, Qi JS, Zhao XD, et al. 2018 Springback prediction of aluminum alloy sheet under changing loading paths with consideration of the influence of kinematic hardening and ductile damage. *Met*. **8** 950
[18] Hemmerich E, Rolfe B, Hodgson PD, et al. 2011 The effect of pre-strain on the material behavior and the Bauschinger effect in the bending of hot rolled and aged steel. *Mater. Sci. Eng. A* **528**(9) 3302
[19] Peng J, Li KS, Peng J, et al. 2018 The effect of pre-strain on tensile behavior of 316L austenitic stainless steel. *Mater. Sci. Technol*. **34**(5) 547
[20] Chen JS, E DX, Zhang JW. 2013 Study on the mechanical property of 5754 aluminum alloy sheet and St15 cold-rolled steel sheet for automobiles. *Auto. Technol. Mater*. **1** 43
[21] She CF, E DX, Lin F. 2013 Analysis on forming properties of bake-hardening sheet steel BH340 and deep-drawing sheet steel St15 for the automobile. *J. Netshape Form. Eng*. **5**(3) 6
[22] Wu JX, Wang Y, Chapuis A, et al. 2019 Microstructure and texture evolution of commercially pure titanium sheet during cold rolling and annealing. *J. Chongqing Univ*. **42**(8) 67
[23] Forcellese A, Fratini L, Gabrielli F, et al. 1998 The evaluation of springback in 3D stamping and coining processes. *J. Mater. Process. Technol*. **80** 108
[24] Huang YM. 2007 Finite element analysis on the V-die coining bend process of steel metal. *Int. J. Adv. Manuf. Technol*. **34** 287
[25] Zong YY, Liu P, Guo B, et al. 2014 Springback evaluation in hot v-bending of Ti-6Al-4V alloy sheets. *Int. J. Adv. Manuf. Technol*. **541** 60
[26] Roth A, Lebyodkin MA, Lebedkina TA, et al. 2014 Mechanisms of anisotropy of mechanical properties of α-titanium in tension conditions. *Mater. Sci. Eng. A* **596** 236
[27] Xu F, Yang L, Zhang YC, et al. 2020 Effects of pre-strain on microstructure, texture and mechanical properties of HSLA. *J. Plast. Eng*. **27**(1) 103
[28] Leyens C, Peters M. Translated by Chen Z. 2005 *Titanium and titanium alloy*. Beijing: Chemical Industry Press 4
[29] Chen FK, Chiu KH. 2005 Stamping formability of pure titanium sheets. *J. Mater. Process. Technol*. **170** 181
[30] Itoh N, Diao GF. 1984 Stamping ability of commercially pure titanium at warm working temperature. *Rare Metal Mater. Eng*. **4** 13
[31] Feng J, Song KX, He JL, et al. 2020 Study on microstructure and properties of Cu-1Ag Alloy microwire in a multi-pass drawing. *Foundry Technol*. **41**(11) 1020